*Erschienen in: 31st European Photovoltaic Solar Energy Conference and Exhibition : proceedings of the international conference held in Hamburg, Germany, 14 September - 18 September 2015. - München : WIP, 2015. - S. 1305-1309. - ISBN 3-936338-39-6*
*https://dx.doi.org/10.4229/EUPVSEC20152015-3DV.2.20*

# INFLUENCE OF DEPOSITION PARAMETERS ON ELEMENTAL CONCENTRATIONS, ELECTRICAL, AND OPTICAL PROPERTIES OF MAGNETRON CO-SPUTTERED AL-DOPED ZNO FILMS

Angelika Gorgulla, Dominik-Pascal Ertel, Giso Hahn, Barbara Terheiden
University of Konstanz, Department of Physics, 78457 Konstanz, Germany
Phone: +49 7531 88 2080, Fax: +49 7531 88 3895, Email: angelika.gorgulla@uni-konstanz.de

ABSTRACT: We investigate the influence of various deposition parameters on Zn and Al elemental concentrations in relation to their effect on the optical and electrical properties of co-sputtered Al-doped zinc oxide (ZnO:Al) films. To determine the Al and Zn concentrations Inductively Coupled Plasma Optical Emission Spectrometry (ICP-OES) is applied. It is shown, that the Al doping concentration $c_{Al}$ strongly depends on the deposition parameters and has a strong influence on the charge carrier density of the films. High Al concentrations of $6.4 \cdot 10^{20}$ and $8.5 \cdot 10^{20}$ $cm^{-3}$ are obtained at increased sputtering temperature (450°C) and reduced oxygen flow (6 sccm), respectively, allowing charge carrier densities $N_e$ up to $2.2 \cdot 10^{20}$ $cm^{-3}$ and electrical resistivities below $2.0 \cdot 10^{-3}$ Ωcm. However, as opposed to an increased sputtering temperature, a low oxygen flow significantly reduces the film transparency. The working pressure appears to have a less profound impact on the Al concentration, but more on the charge carrier mobility and defect density within the films: an increase from 0.5 to 1.5 mTorr decreases the ratio $N_e/c_{Al}$, which is a measure for the defect density, by a factor of seven and simultaneously leads to a decrease of mobility from 29 to 2 $cm^2V^{-1}s^{-1}$. XRD measurements indicate, that higher working pressure leads to poorer crystallinity.
Keywords: TCO, AZO, ZnO:Al, heterojunction solar cells, magnetron sputtering

## 1 INTRODUCTION

Al-doped zinc oxide (ZnO:Al) thin films are of interest in numerous photovoltaic applications due to their features such as a high transmittance within the ultraviolet, visble and near-infrared ranges as well as low electrical resistivity in the order of $10^{-3}$ to $10^{-4}$ Ωcm. In recent years, the heterojunction solar cell concept has attracted much attention as it allows high conversion efficiencies above 20% in an industrial-production. Key advantage of heterojunction solar cells is the high open circuit voltage above 730 mV, which can be attributed to the excellent passivation quality of the amorphous silicon used as emitter and back surface field (BSF) layer. Due to the low electric conductivity of a-Si:H, a transparent conducting oxide (TCO) is needed at the front side of these solar cells in order to maintain a high lateral conductivity of the emitter layer. ZnO:Al as TCO is a promising alternative for the still widely used, but much more costly indium tin oxide (ITO).

While numerous studies exist investigating the effects of deposition parameters on optical, structural and electrical ZnO:Al films, there is no comprehensive study to our knowledge investigating systematically the effect of the deposition parameters on the elemental concentrations (Zn, Al) of magnetron sputtered ZnO:Al films. Purpose of this study is therefore to investigate the effect of various deposition parameters (oxygen flow, substrate temperature and working pressure) on the elemental concentrations in association with their impact on the optical and electrical film properties. To obtain the Al and Zn concentrations inductively coupled plasma optical emission spectrometry (ICP-OES) [1] is used, which is a novel approach of investigating element concentrations in ZnO thin films [2].

## 2 EXPERIMENTAL

ZnO:Al films were deposited on float-zone Si (for ellipsometry measurements) and borofloat glass (for all remaining measurements) at room temperature in a radio-frequency rf-13.56 MHz magnetron sputtering system (ATC-2200, AJA International) by reactive co-sputtering using metallic Zn (300 W) and Al targets (255 W) of 99.99% purity.

To systematically investigate the influence of deposition parameters on the film properties, four sets of films were prepared by changing a specific deposition parameter at a time, with the others remaining constant. The $O_2$ flow was varied from 6 to 9 sccm, the substrate temperature from 25 to 450°C and the working pressure from 0.5 to 1.5 mTorr. Unless noted otherwise, the sputtering parameters were 25°C substrate temperature, 7.5 sccm oxygen flow and 0.5 mTorr working pressure.

Prior to the sputtering process, all substrates were ultrasonically cleaned in acetone, isopropanol and deionized water sequentially. Afterwards, the substrates were dried with nitrogen gas. Before deposition, the sputtering chamber was evacuated to a base pressure of less than $10^{-6}$ Torr. After a pre-sputtering period of 2 min under deposition conditions, the sputtering deposition was performed. During deposition, the substrates were rotated with constant speed for film uniformity.

Electrical resistivity, free carrier density and carrier mobility of the films were derived from Hall measurements at room temperature using the van der Pauw method. Optical properties were characterized by spectral transmission and reflection measurements within a wavelength range of 300-2500 nm taken by a spectral photometer. The optical constants (n, k) and optical bandgaps $E_{gap}$ were deduced from spectral ellipsometry measurements between 250 and 1100 nm. The optical band gap $E_{gap}$ was calculated from the fitted data by using Tauc's formula [3]. For ICP-OES (720 series, Agilent) element analysis, the ZnO:Al films were dissolved in 0.5%$_{abs}$ hydrofluoric acid. To guarantee accurate ICP-OES measurements with element concentrations above quantification limit, the thickness of the deposited films was in the range of 300 to 1000 nm as verified by profilometric measurements. The ratio of Zn and O was determined by energy dispersive X-ray spectroscopy (EDX) measurements. The crystalline structure of the films was analyzed by X-ray diffraction (XRD) (D8 XRPD, Bruker) using Cu $K_\alpha$ radiation (0.1542 nm). The mean grain size of the films is derived from Scherrer's equation [4] using the (002) diffraction peak.

## 3 RESULTS AND DISCUSSION

### 3.1 Substrate temperature

Charge carrier density $N_e$, Al concentration $c_{Al}$ and the doping concentration $N_D$ deduced from the element concentrations (Zn and Al) and the ratio of Zn and O are shown in Fig. 1. As was to be expected, $c_{Al}$ and $N_e$ are correlated. The highest Al concentration of $6.4 \cdot 10^{20}$ cm$^{-3}$ (0.41 %$_{at}$) is obtained at 450°C and yields the highest carrier density of $1.4 \cdot 10^{20}$ cm$^{-3}$.

However, the fraction of Al atoms effectively acting as dopants, which is given by the ratio $N_e/c_{Al}$, decreases from 0.25 to 0.16 as the substrate temperature is increased from 250 to 450°C (Fig. 2). There are two possible reasons. Firstly, an increased fraction of Al atoms is not incorporated into the ZnO matrix as dopants, e.g. as substitutional atoms on Zn lattice sites, but for example as interstitials inducing defects. Secondly, an increased fraction of charge carriers introduced by Al dopants is compensated by other extrinsic or intrinsic defects. The ratio $N_e/c_{Al}$ can therefore be seen as a measure for the defect density within the films. The drop in electron mobility $\mu_e$ at high deposition temperatures above 200°C (Fig. 2) may be caused by enhanced impurity scattering due to an increased defect density at elevated temperatures. The decrease of the mobility below 200°C is presumably a consequence of a reduced crystallinity, which can be observed by XRD measurements.

The intensity of the (002) diffraction peak and the mean grain size derived from Scherrer's equation [4] with an approximate error of less than 5% are depicted in Fig. 3.

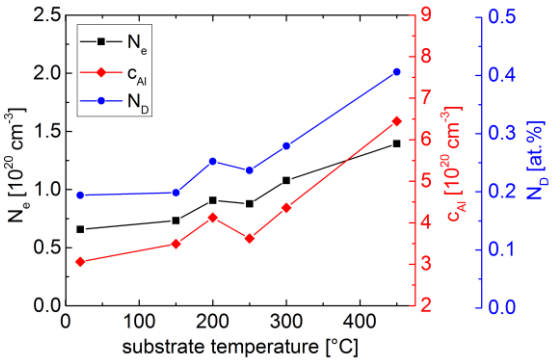


**Figure 1:** Charge carrier density $N_e$, Al concentration $c_{Al}$ and doping concentration $N_D$ versus substrate deposition temperature.

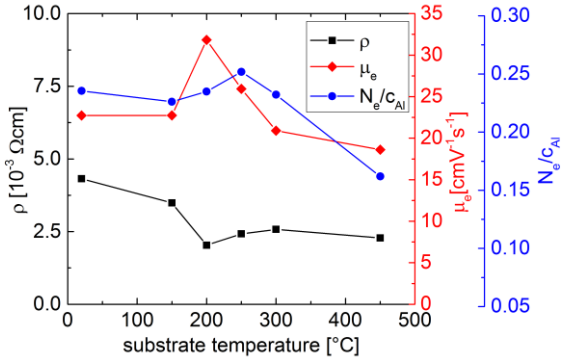


**Figure 2:** Electrical resistivity ρ, mobility $\mu_e$ and fraction of Al atoms effectively acting as donors $N_e/c_{Al}$ versus substrate deposition temperature.

Below 200°C, the (002) peak intensity significantly decreases and grain size reduces from 49 to below 45 nm. The reason for the reduced crystallinity is presumably, that at lower substrate temperatures the sputtered atoms cannot obtain enough heat energy from the substrate surface in order to obtain optimum bonding lengths and directions to the adjacent substrate and film atoms [5]. The reduced crystallinity leads to enhanced grain boundary scattering.

The electric resistivity is depicted in Fig. 2. A substrate temperature of 200°C is favorable for producing low resistivity films, $\leq 2.0 \cdot 10^{-3}$ Ωcm.

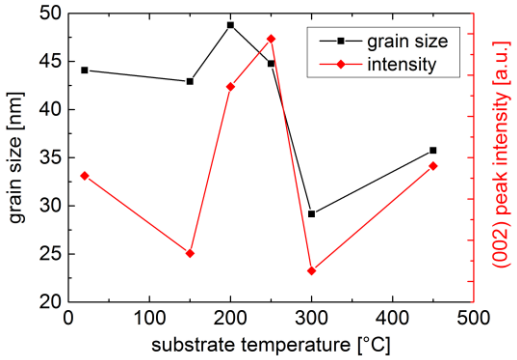


**Figure 3:** (002) peak intensity of XRD spectra and grain size derived from Scherrer's equation in dependence of substrate deposition temperature.

Optical transmission in the long-wavelength (> 2000 nm) range decreases slightly with increased deposition temperature, which is a result of enhanced free carrier absorption. The optical bandgap increases monotonously from 3.20 to 3.41 eV (Fig. 4) due to the Burstein-Moss-effect, which results in a distinct blue-shift in the transmission spectra at 450°C. The optical transmittance weighted by ASTM G173-03 solar spectrum within a wavelength range relevant for solar cells (300-1100 nm) increases slightly from 79% at 25°C to 84% at 450°C deposition temperature.

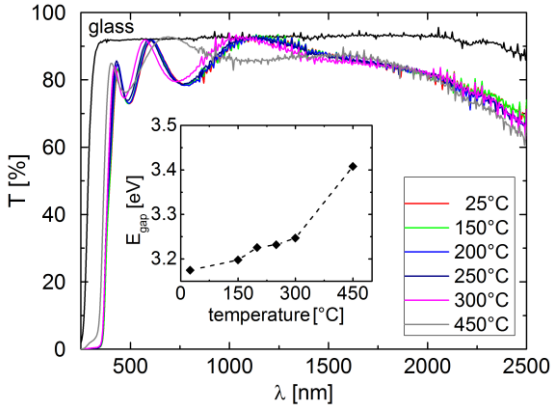


**Figure 4:** Optical transmission spectra and optical band gap energies for various substrate deposition temperatures.

### 3.2 Oxygen flow

Highest $N_e$ ($2.2 \cdot 10^{20}$ cm$^{-3}$) and $c_{Al}$ ($8.5 \cdot 10^{20}$ cm$^{-3}$) are obtained at a low $O_2$ flow of 6 sccm (Fig. 5). At higher $O_2$ flow, $N_e$ and $c_{Al}$ decrease monotonously down to $7.6 \cdot 10^{19}$ cm$^{-3}$ and $3.9 \cdot 10^{20}$ cm$^{-3}$ at 9 sccm, respectively. Doping concentration $N_D$ decreases from 0.47 to 0.17 %$_{at}$. $N_e/c_{Al}$ decreases slightly for fluxes below 6.5 sccm (Fig. 6) and indicates an increase of defects. This increase can be

attributed to the very high doping concentration at 6 sccm, which leads to more structural disorder and therefore a reduction of mobility (Fig. 6).

The monotonous decrease of $N_e/c_{Al}$ at $O_2$ flows above 6.5 sccm on the other hand, may be caused by a decrease of oxygen vacancies. Oxygen vacancies can act as doubly charged electron donators and therefore contribute to the formation of free charge carriers [6]. Interstitial oxygen may be responsible for the decrease of electric mobility above 8 sccm (Fig. 6), as it can act as trap center for free carriers and become a dominating defect in ZnO [7].

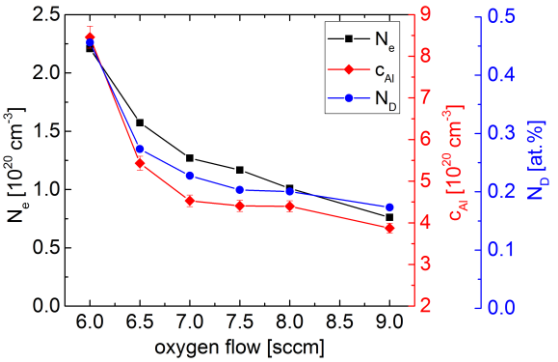


**Figure 5:** Charge carrier density $N_e$, Al concentration $c_{Al}$ and doping concentration $N_D$ versus oxygen flow.

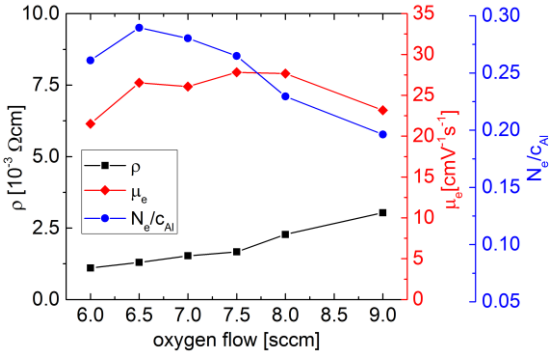


**Figure 6:** Electrical resistivity ρ, mobility $\mu_e$ and fraction of Al atoms effectively acting as donors $N_e/c_{Al}$ versus oxygen flow.

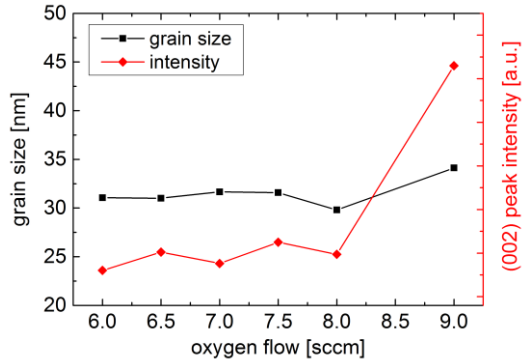


**Figure 7:** (002) peak intensity of XRD spectra and grain size derived from Scherrer's equation in dependence of oxygen flow.

Despite the decreased mobility above 8 sccm, a slightly improved film crystallinity can be observed; while the grain size stays almost constant within the margins of error at around 32 nm and increases slightly at 9 sccm, the (002) peak intensity increases significantly (Fig. 7). The reason for this increase remains unclear.

In the transmission spectra in Fig. 8 it can be observed, that a decreased $O_2$ flow significantly reduces film transparency. This suggests, that at lower $O_2$ flow less oxygen is incorporated into the film. As the $O_2$ flow is increased, transmission between 490 and 530 nm increases, which can be attributed to a decrease of oxygen vacancies [8]. In the long-wavelength range (> 1000 nm), transmission increases with higher $O_2$ flow due to reduced free carrier absorption. The optical bandgap stays constantly within error margins at around 3.3 eV (not shown). The optical transmittance weighted by ASTM G173-03 solar spectrum within a wavelength range relevant for solar cells (300-1100 nm) increases significantly as $O_2$ flow is increased from 17% at 6 sccm to 76% at 9 sccm (Fig. 9). For optimal optoelectronic film properties a trade-off is therefore necessary between high transparency (high $O_2$ flow) and low resistivity (low $O_2$ flow).

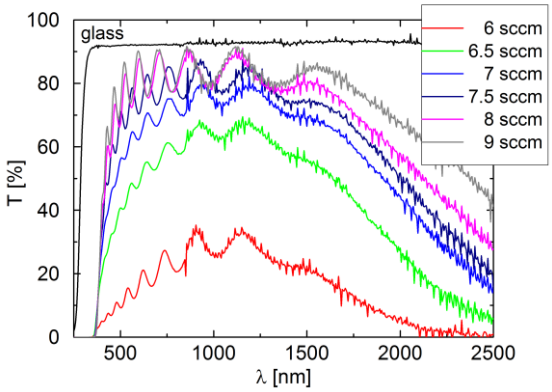


**Figure 8:** Optical transmission spectra for various oxygen flows.

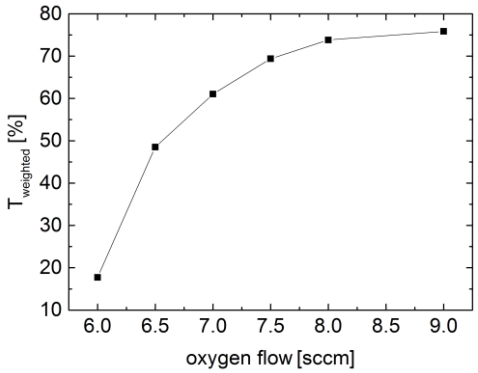


**Figure 9:** Optical transmission weighted by ASTM G173-03 solar spectrum in the range of 300-1100 nm versus oxygen flow.

### 3.3. Working pressure

The working pressure has less influence on $c_{Al}$ and $N_e$ compared to oxygen flow and substrate temperature. Both decrease monotonously within the pressure range from 0.5 to 1.5 mTorr (Fig. 10). However, $N_e/c_{Al}$ drops considerably from 0.27 to 0.07 and the charge carrier mobility from 29 to 2 $cm^2V^{-1}s^{-1}$ (Fig. 11). There are two possible reasons: firstly, a high working pressure increases the collision frequency of the sputtered particles and $Ar^+$ ions, which leads to an increased energy loss of the

sputtered particles before colliding with substrate or film surface and hence leaves less energy for the particles to obtain optimum bonding configuration with the adjacent film atoms. This results in a reduced crystallinity and decreased mobility. Secondly, higher working pressure allows more $Ar^+$ ions to participate in the charge carrier transport and results in a higher current. As the power is the product of current and voltage and kept constant, the voltage applied between target and substrate is decreased. This again decreases the energy of the sputtered particles and leads to poorer crystallinity and lower mobility [9]. The reduced crystallinity is reflected in a reduction of grain size from above 30 nm at 0.5 mTorr to below 23 nm at 1.5 mTorr and in a decrease of (002) peak intensity at working pressure above 0.75 mTorr (Fig. 12).

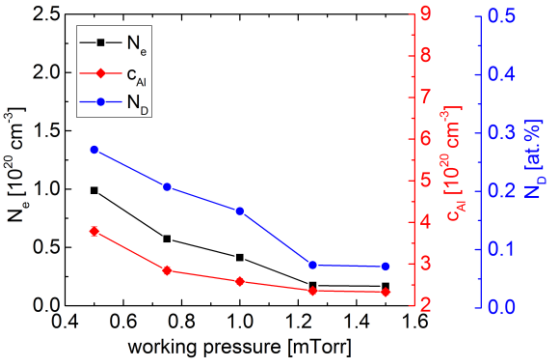


**Figure 10:** Charge carrier density $N_e$, Al concentration $c_{Al}$ and doping concentration $N_D$ versus working pressure.

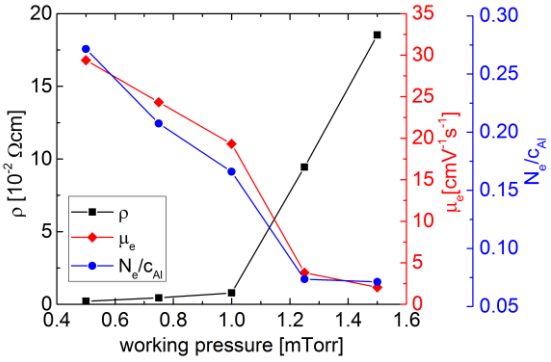


**Figure 11:** Electrical resistivity ρ, mobility $\mu_e$ and fraction of Al atoms effectively acting as donors $N_e/c_{Al}$ versus working pressure.

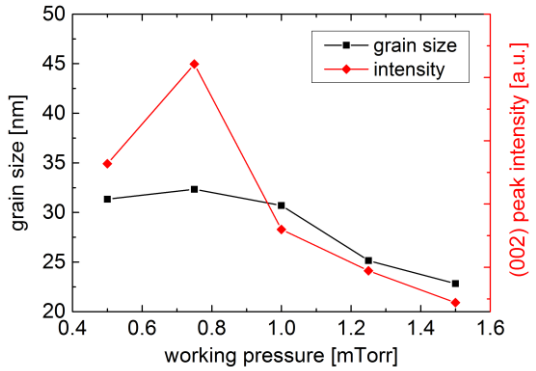


**Figure 12:** (002) peak intensity of XRD spectra and grain size derived from Scherrer's equation in dependence of working pressure.

Reduced carrier density and mobility result in an increase of electrical resistivity of about two orders of magnitude as the working pressure is increased from 0.5 to 1.5 mTorr (Fig. 11). Low working pressure is therefore clearly beneficial for producing highly conductive films. However, when the working pressure is too low, the Ar plasma becomes difficult to discharge and unstable during film deposition.

The transmission spectra and optical bandgaps for various working pressures are shown in Fig. 13. In the long-wavelength (> 2000 nm) range, the optical transmission decreases with lower working pressure as a consequence of enhanced free carrier absorption. The optical bandgap decreases from 3.41 eV at 0.5 mTorr to below 3.50 eV above 1.0 mTorr due to the Burstein-Moss-effect.

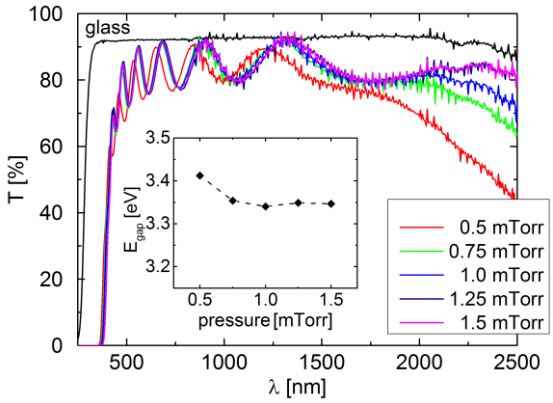


**Figure 13:** Optical transmission spectra and optical band gap energies for various working pressures.

## 4 CONCLUSIONS

We have investigated the impact of various deposition parameters on the element concentrations of ZnO:Al films by ICP-OES, a novel and relatively simple approach for a high throughput investigation of element concentrations in ZnO films. It has been found, that the Al doping concentration mostly determines the charge carrier density, while the charge carrier mobility is strongly influenced by the defect density of the films. In conclusion, the Al doping concentration is of major importance for the understanding as well as optimization of optical and electrical film properties.

## ACKNOLEDGEMENTS

Part of this work was financially supported by the German Federal Ministry for Economic Affairs and Energy (FKZ 0325581) and within the "REFINE" project from the Carl-Zeiss-Stiftung. The content is the responsibility of the authors.

## REFERENCES

[1] S. Ghosh et al., Asian J. Pharm. Ana. 3 (2013) 24.
[2] A. Gorgulla et al., Energy Procedia 77 (2015), 687.
[3] J. Tauc et al., J. Non-Cryst. Solids 8 (1979) 569.
[4] P. Scherrer, Göttinger Nachrichten Gesellschaft. 2 (1918) 98.

[5] A.I. Ali et al., J. Korean Phys. Soc. 49 (2006) S652.
[6] R. Vidya et al., Phys. Rev. B 83 (2001) 45206.
[7] K. E. Knutsen et al., Phys. Rev. B 86 (2012) 121203.
[8] H. S. Kang et al., J. Appl. Phys. 95 (2004) 1246.
[9] D. H. Zhang et al., Appl. Surf. Sci. 158 (2000) 43.